AGU PUBLICATIONS

Water Resources Research

RESEARCH ARTICLE
10.1002/2014WR015602

Incorporation of groundwater pumping in a global Land Surface Model with the representation of human impacts

Yadu N. Pokhrel[1], Sujan Koirala[2], Pat J.-F. Yeh[3], Naota Hanasaki[4], Laurent Longuevergne[5], Shinjiro Kanae[6], and Taikan Oki[7]

[1]Department of Civil and Environmental Engineering, Michigan State University, East Lansing, Michigan, USA, [2]Deparment of Biogeochemical Integration, Max Planck Institute for Biogeochemistry, Jena, Germany, [3]Department of Civil and Environmental Engineering, National University of Singapore, Singapore, [4]National Institute for Environmental Studies, Tsukuba, Japan, [5]UMR CNRS 6118—Géosciences Rennes, Université de Rennes, Rennes, France, [6]Department of Civil Engineering, Tokyo Institute of Technology, Tokyo, Japan, [7]Institute of Industrial Science, University of Tokyo, Tokyo, Japan

Key Points:
- Global Land Surface Model with human impacts, groundwater dynamics, and pumping
- Explicitly simulated groundwater withdrawal and depletion
- Groundwater depletion in the Central Valley and the High Plains

Supporting Information:
- Pokhrel_WRR2014_Auxiliaryreadme
- 2014WR015602_fs01
- 2014WR015602_fs02
- 2014WR015602_fs03
- 2014WR015602_fs04
- 2014WR015602_fs05
- 2014WR015602_fs06
- 2014WR015602_fs07a
- 2014WR015602_fs07b
- 2014WR015602_ts01
- 2014WR015602_ts02
- 2014WR015602_text01

Correspondence to:
Y. N. Pokhrel,
ypokhrel@egr.msu.edu

Citation:
Pokhrel, Y. N., S. Koirala, P. J.-F. Yeh, N. Hanasaki, L. Longuevergne, S. Kanae, and T. Oki (2015), Incorporation of groundwater pumping in a global Land Surface Model with the representation of human impacts, *Water Resour. Res.*, *51*, 78–96, doi:10.1002/2014WR015602.

Received 19 MAR 2014
Accepted 16 NOV 2014
Accepted article online 24 NOV 2014
Published online 8 JAN 2015

Abstract Observations indicate that groundwater levels are declining in many regions around the world. Simulating such depletion of groundwater at the global scale still remains a challenge because most global Land Surface Models (LSMs) lack the physical representation of groundwater dynamics in general and well pumping in particular. Here we present an integrated hydrologic model, which explicitly simulates groundwater dynamics and pumping within a global LSM that also accounts for human activities such as irrigation and reservoir operation. The model is used to simulate global water fluxes and storages with a particular focus on groundwater withdrawal and depletion in the High Plains Aquifer (HPA) and Central Valley Aquifer (CVA). Simulated global groundwater withdrawal and depletion for the year 2000 are 570 and 330 km^3 yr^{-1}, respectively; the depletion agrees better with observations than our previous model result without groundwater representation, but may still contain certain uncertainties and is on the higher side of other estimates. Groundwater withdrawals from the HPA and CVA are ~22 and ~9 km^3 yr^{-1}, respectively, which are also consistent with the observations of ~24 and ~13 km^3 yr^{-1}. The model simulates a significant decline in total terrestrial water storage in both regions as caused mainly by groundwater storage depletion. Groundwater table declined by ~14 cm yr^{-1} in the HPA during 2003–2010; the rate is even higher (~71 cm yr^{-1}) in the CVA. These results demonstrate the potential of the developed model to study the dynamic relationship between human water use, groundwater storage, and the entire hydrologic cycle.

1. Introduction

Today, at least one-fourth of the world's population relies heavily on groundwater (GW) [*Jackson et al*., 2001; *Alley et al*., 2002], and it is likely that the dependence on GW will continue to grow in the following decades due to the increase in population and associated demands for water [*Vörösmarty et al*., 2000; *Rosegrant and Cai*, 2002; *Gleick*, 2003; *Oki and Kanae*, 2006]. These issues have raised concerns about GW sustainability [*Gleick and Palaniappan*, 2010; *Gleeson et al*., 2012; *Taylor et al*., 2013], particularly in the major agricultural regions such as the High Plains Aquifer (HPA) and the Central Valley Aquifer (CVA) which are extensively irrigated by GW [*Scanlon et al*., 2012a]. Human exploitation of GW dates back to the early civilizations [*Postel*, 1999], but the extensive GW exploitation began only during the last century owing to the rapid expansion of irrigated croplands [*Shah et al*., 2007; *Giordano*, 2009; *Wada et al*., 2011]. Increased use of GW—the readily available and generally high-quality source of freshwater—has facilitated improvement in livelihoods, increase in agricultural productivity, food security, economic growth, and human adaptability to climate variability in many regions [*Giordano*, 2009; *Shah et al*., 2007]. However, these astounding benefits of GW as a resource have often come with certain unanticipated negative environmental consequences such as aquifer depletion, water quality deterioration, and degradation of ecosystems [*Sahagian et al*., 1994; *Morris et al*., 2003; *Gleick*, 2003; *Giordano*, 2009; *Shah et al*., 2007; *Konikow and Kendy*, 2005; *Foster and Chilton*, 2003; *Sophocleous*, 2002; *Schwartz and Ibaraki*, 2011]. Recent studies have shown that GW levels have been declining at an alarming rate in many regions around the world [e.g., *Rodell et al*., 2009; *Wada et al*., 2010; *Famiglietti et al*., 2011; *Pokhrel et al*., 2012a; *Döll et al*., 2014] owing to increased use of GW at the rate exceeding its natural replenishment [*Giordano*, 2009; *Shah et al*., 2007].

As concerns over GW sustainability keep growing, the importance of identifying and solving GW problems has become increasingly apparent [e.g., *Gleick*, 2003; *Giordano*, 2009; *Shah et al*., 2007]. The lack of global observations, however, still limits our understanding of the dynamic relationship between GW and the hydrologic cycle [*Alley et al*., 2002; *Taylor et al*., 2013], which are both changing continually in response to climatic and human-induced stresses [*Postel et al*., 1996; *Rockström et al*., 2009; *Nilsson et al*., 2005; *Vörösmarty et al*., 2000]. While the in situ observations of GW level (storage) are still quite limited globally, the Gravity Recovery and Climate Experiment (GRACE) satellite mission [*Tapley et al*., 2004] launched in 2002 has provided a new source of information of the terrestrial water balance which can be used to estimate the changes in terrestrial water storage (TWS) over time [e.g., *Alsdorf and Lettenmaier*, 2003; *Lettenmaier and Famiglietti*, 2006; *Rodell et al*., 2009].

Changes in TWS inferred from GRACE observations have been used to monitor GW storage change [e.g., *Yeh et al*., 2006; *Rodell et al*., 2009; *Longuevergne et al*., 2010; *Famiglietti et al*., 2011; *Döll et al*., 2012, 2014; *Scanlon et al*., 2012b]. However, since GRACE measures only the overall changes in the vertically integrated total water storage, the changes in GW storage alone cannot be estimated by using the TWS inferred from GRACE. To overcome this shortcoming in the estimation of individual TWS components, some auxiliary data on the other relevant storage compartments (e.g., surface water, soil moisture, and snow storages), which are usually obtained from in situ observations or estimated using Land Surface Model (LSM) simulations, have to be used as a priori to obtain the desired TWS component. For example, GW storage change is estimated by deducting the changes in surface water and soil moisture storages obtained from in situ observations [e.g., *Yeh et al*., 2006; *Strassberg et al*., 2009; *Scanlon et al*., 2012b] or models [e.g., *Rodell et al*., 2009; *Famiglietti et al*., 2011], but this may involve certain inconsistency since GRACE data and model results are two independent products. LSMs simulate various TWS components; however, since most state-of-the-art global LSMs do not explicitly simulate GW processes and human impacts, the changes in GW storage associated with human water use cannot be consistently simulated within a single model framework. In many previous global-scale LSM studies, GW storage was considered only implicitly by lumping it into either soil moisture [e.g., *Rodell et al*., 2004] or river water storage [e.g., *Kim et al*., 2009; *Alkama et al*., 2010].

Although there have been increasing number of studies highlighting the significance of GW representation in LSMs [e.g., *Yeh and Eltahir*, 2005a, 2005b; *Maxwell and Miller*, 2005; *Fan et al*., 2007; *Niu et al*., 2007; *Lo and Famiglietti* [2010]; *Miguez-Macho and Fan*, 2012; *Koirala et al*., 2014], these studies simulate the natural flow of water without taking into account the impacts of human activities. There are other models capable of simulating surface and subsurface water flow processes including lateral groundwater transport while also accounting for irrigation management and groundwater pumping [e.g., *Faunt*, 2009; *Ferguson and Maxwell*, 2012; *Condon and Maxwell*, 2014], but these models are particularly designed for catchment to regional-scale applications. Thus, representing human impacts in large-scale LSMs still remains as one of the major challenges in hydrology [*Wood et al*., 2011]. It is important to note that LSM here refers to the models that are an integral component of the General Circulation Models (GCMs) as opposed to the hydrological models designed for offline simulations. Some studies have incorporated irrigation into the LSMs [e.g., *de Rosnay et al*., 2003; *Ozdogan et al*., 2010; *Sorooshian et al*., 2011; *Lo and Famiglietti*, 2013; *Leng et al*., 2013], but they have mainly focused on irrigation water demand without considering water withdrawals and the associated alterations of the water cycle.

There are numerous other global or continental-scale studies which have incorporated human impacts into the global hydrological models [*Alcamo et al*., 2003; *Haddeland et al*., 2006; *Rost et al*., 2008; *Hanasaki et al*., 2008; *Wisser et al*., 2010; *van Beek et al*., 2011; *Pokhrel et al*., 2012b; *Döll et al*., 2012; *Wada et al*., 2011, 2014; *Voisin et al*., 2013], but most of them do not simulate relevant GW processes such as the water table dynamics and GW pumping. One exception is the model developed by *Döll et al*. [2012] which can differentiate between the water withdrawn from surface water and GW and thus can estimate the changes in GW storage; however, the GW store was simulated as a linear reservoir without considering two-way interactions with soil moisture. Therefore, the lack of water table dynamics limits the simulation of soil moisture-groundwater interactions, an important mechanism for sustaining summertime evapotranspiration, which has been confirmed by various previous studies [e.g., *Yeh and Famiglietti*, 2009]. The model developed by *Wada et al*. [2011, 2014] also estimates GW depletion based on the country-scale statistical data of GW withdrawal and simulated recharge, but without taking into account the two-way interactions between soil moisture and groundwater.

In this study, we develop an integrated hydrological model that explicitly simulates GW withdrawal and storage change within an internally consistent framework in terms of the water balance, thus providing a new opportunity to independently estimate GW depletion and all relevant components of TWS without using a priori information. We refer to the model as an integrated model as it integrates modules representing various natural and human-induced processes together into a single, consistent modeling framework. The model is developed by representing the water table dynamics and GW pumping within our previously developed model that accounts for human activities such as irrigation, reservoir operation, and human water withdrawal within a global LSM [*Pokhrel et al*., 2012b, hereafter *P12b*]. Here the unique feature of the new model is that it simulates the water table dynamics as well as GW pumping and other human water withdrawals simultaneously within the consistent framework of a global LSM.

In the following, section 2 provides the model description and data with the emphasis on the GW model and the new pumping scheme. Model evaluation and discussion of results are given in section 3, which first presents the evaluation of simulated river discharge, irrigation water requirements, and GW withdrawal and depletion against the available observations worldwide, then the details of GW withdrawals in the principal aquifers in the United States (U.S.), and finally the simulation results of GW depletion in the HPA and CVA. These two particular aquifers are selected for several reasons. First, they are located within the most important agricultural regions in the U.S. and the world, and the GW levels have been reported to be continuously declining over the past decades in both aquifers [*Faunt*, 2009; *McGuire*, 2011; *Famiglietti et al*., 2011; *Scanlon et al*., 2012a, 2012b]. The HPA and CVA rank first and second respectively for GW withdrawal among all aquifers in the US [*Maupin and Barber*, 2005]. Second, both aquifers are regularly monitored by the United States Geological Survey (USGS) and therefore are highly data rich in terms of GW monitoring [*McGuire*, 2011; *Faunt*, 2009; *Scanlon et al*., 2012a; *Strassberg et al*., 2009]. And third, the choice of the HPA is also facilitated by the large areal extent (450,000 km^2), which makes it suitable for the application of GRACE data. Finally, section 4 summarizes the findings from this study and provides concluding remarks and future research directions.

2. Model Description and Data

The model presented in this study comprises of Human Impact (Hi) modules (e.g., reservoir operation, crop and irrigation, water withdrawal) and a GW (GW) dynamics and pumping schemes with a global LSM called the Minimal Advanced Treatments of Surface Interaction and Runoff (MATSIRO) [*Takata et al*., *2003*], thus the new model is termed as HiGW-MAT. The human impact modules were incorporated into the MATSIRO in our previous work [*P12b*]. In the present study, we enhance the model developed by *P12b* through the representation of the water table dynamics originally proposed by *Yeh and Eltahir* [2005a, 2005b] at the regional scale and incorporated into the global-scale LSM by *Koirala et al*. [2014]. Then, we develop and incorporate a new GW pumping scheme within the water withdrawal and GW dynamics modules. The model provides the first opportunity to explicitly simulate GW withdrawal, recharge, and depletion within a consistent modeling framework. Description of different modules in HiGW-MAT with a particular emphasis on the formulations of the pumping scheme is provided in the following.

2.1. The MATSIRO LSM

MATSIRO [*Takata et al*., 2003] is an LSM developed to compute biophysical exchanges in the GCM called MIROC (the Model for Interdisciplinary Research on Climate) [*Hasumi and Emori*, 2004; *Watanabe et al*., 2010]. MATSIRO estimates the exchange of energy, water vapor, and momentum between the land surface and the atmosphere on a physical basis. Effects of vegetation on the surface energy balance are calculated on the basis of the multilayer canopy model of *Watanabe* [1994] and the photosynthesis-stomatal conductance model of *Collatz et al*. [1991]. The soil column, which has a total thickness of 4 m, is divided into five layers (5, 20, 75, 100, and 200 cm from top to bottom). The vertical movement of soil moisture is estimated by numerically solving the Richards equation [*Richards*, 1931] for all soil layers without considering the location of water table depth (WTD) because there is no explicit representation of the saturated zone. A simplified TOPMODEL [*Beven and Kirkby*, 1979; *Stieglitz et al*., 1997] is used to represent surface and subsurface runoff processes.

2.2. The Human Impact Modules

Detailed description of the human impact schemes and model validation can be found in *P12b*; for completeness, here we provide a brief summary of the model. Modules representing various human activities

(reservoir operation, crop growth, irrigation, water withdrawal, and environmental flow requirements) were incorporated within MATSIRO LSM in a consistent manner such that the model simulates the natural flow of water globally while taking into account the human factors. Because the original MATSIRO does not account for runoff routing, a river routing model (Total Runoff Integrating Pathways, TRIP) [*Oki and Sud*, 1998] was also incorporated into the modeling framework. Subgrid variability of vegetation is represented by partitioning each grid cell into two tiles: natural vegetation and irrigated cropland. The crop growth module, based on the crop vegetation formulations and parameters of the Soil and Water Integrated Model (SWIM [*Krysanova et al*., 1998]), estimates the cropping period necessary to obtain mature and optimal total plant biomass for 18 different crop types. Irrigation water demand is estimated based on the soil moisture deficit in the top meter of the soil column as,

$$I = \frac{\rho_w}{\Delta t} \sum_{k=1}^{3} \{max[(TSMC - \theta_k), 0] D_k\} \quad (1)$$

where *TSMC*, given as $\alpha \times \theta_s$, is the target soil moisture content, I [kg m^{-2} s^{-1}] is the irrigation demand; ρ_w [kg m^{-3}] is the density of water; Δt is model time step; θ_s and θ_k [m^3 m^{-3}] are the soil moisture content at field capacity and simulated actual soil moisture content, respectively; and D_k [m] is the thickness of k_{th} soil layer from the land surface. The α is set at 1 for rice and 0.75 for other crops (see *P12b* for details).

The model routes the simulated surface and subsurface runoff through the digital river networks of TRIP. The operation module of the reservoirs, located on the river networks, is activated for grid cells containing a reservoir. The reservoir operation module, based on *Hanasaki et al*. [2006], targets the maximum storage to be 85% of the storage capacity for the large reservoirs. The medium-sized reservoirs with the storage capacity ranging from 3×10^6 to 1×10^9 m^3 [*Hanasaki et al*., 2010], however, can be 100% filled with the excess runoff flowing directly to the rivers. The withdrawal module extracts the total (domestic, industrial, and agricultural) water requirements from river channels considering the lower threshold of river discharge prescribed as the environmental flow requirement. While the irrigation demand is simulated by the irrigation module, the domestic and industrial water uses are obtained from the AQUASTAT database of the Food and Agricultural Organization (FAO; http://www.fao.org/nr/water/aquastat/main/index.stm). An option was added to withdraw the total demand of a grid cell from the predefined local sources such as natural streams and medium-sized reservoirs or from an imaginary source if the local sources run out. Thus, the nonrenewable GW use, estimated as the deficit in supply from the near-surface sources to meet the total demand of a grid cell, was obtained from the imaginary source which is identical to the nonrenewable and nonlocal blue water (NNBW), originally proposed by *Rost et al*. [2008] and used by various other studies [e.g., *Hanasaki et al*., 2010; *P12b*] to account for the unsustainable water use from nonrenewable GW. In the new model, this imaginary source of water has been replaced by an explicit GW pumping scheme described in section 2.4.

2.3. GW Representation

The GW scheme, which is based on *Yeh and Eltahir* [2005a], consists of an unconfined aquifer model in which the soil column includes the coupling (two-way interactions) between the unsaturated zone and the underlying unconfined aquifer through the exchange of moisture flux at the water table. A detailed description of the model can be found in *Yeh and Eltahir* [2005a] and *Koirala et al*. [2014]; for completeness, the key formulations are highlighted in Appendix A. The dynamics in WTD is determined by GW recharge and base flow, and the location of the water table is updated at every time step based on the groundwater balance equation (Appendix A, equation (A1)). The dynamic location of the water table determines the exact number of unsaturated soil layers to be resolved numerically by the Richards equation [*Richards*, 1931]. This allows the thickness of unsaturated zone and hence the depth at which the exchange of moisture flux takes place to vary with time. This is physically more realistic than the approach of allowing gravity drainage from the bottom of a fixed-depth soil column as used in most global-scale LSMs. To accommodate the variable WTD accurately, *Koirala et al*. [2014] extended the soil column of MATSIRO to 40 m with 13 layers in total (top three layers of 5, 20, and 75 cm, nine next layers of 1 m, and a bottom layer of 30 m thickness). In this study, the thickness of the bottom layer is increased to 90 m to prevent the drop of the water table below the bottommost soil layer due to GW pumping.

2.4. The New GW Pumping Scheme

In *P12b*, the water demand that is not met by the availability from near-surface sources was fulfilled by NNBW [e.g., *Rost et al*., 2008; *Hanasaki et al*., 2010]. In this study, we replace this imaginary source of NNBW

by the new GW pumping scheme which withdraws water from GW and allows storage replenishment though recharge simulated by the GW dynamics scheme, thus providing a dynamic link between human water withdrawals and the dynamics of surface water-groundwater interactions. The scheme estimates the amount of water to be withdrawn from the aquifers based on the difference between the total demand of a grid cell and the water available from the surface sources such as river channels and reservoirs. The GW pumpage/withdrawal is estimated as,

$$GW_{pt} = CWU_a + CWU_d + CWU_i - WS_{riv} - WS_{Mres} \quad (2)$$

$$CWU_d = f_d \times TWU_d \quad (3)$$

$$CWU_i = f_i \times TWU_i \quad (4)$$

where GW_{pt} [$L\ T^{-1}$] is the total GW pumpage, CWU_a [$L\ T^{-1}$] is the consumptive agricultural water use (i.e., net irrigation demand), CWU_d [$L\ T^{-1}$] is the consumptive domestic water use, and CWU_i [$L\ T^{-1}$] is the consumptive industrial water use. WS_{riv} [$L\ T^{-1}$] and WS_{Mres} [$L\ T^{-1}$] are the water supplied by rivers (including the release from reservoirs in the upstream areas) and medium-sized reservoirs, respectively. TWU_d [$L\ T^{-1}$] and TWU_i [$L\ T^{-1}$] are the total domestic and industrial water uses, respectively. f_d and f_i are the consumptive fractions of total domestic and industrial water uses, which are set to be 10% and 15%, respectively, following *Shiklomanov* [2000]. The pumped water is used for irrigation, domestic, and industrial purposes. For the domestic and industrial water withdrawals, the nonconsumptive fraction is assumed to flow back to GW as return flow. Irrigation water, however, enters into soil water storage and its ultimate fate is determined by land surface water and energy balances.

The water balance of a grid cell with GW pumping can be explained by separating the soil column into the unsaturated (vadose) zone and GW reservoir (see supporting information Figure S1). The water balance of the GW reservoir can be expressed in terms of the net GW recharge (R_{gw} [$L\ T^{-1}$]), defined as the gravity drainage flux less the capillary flux near the water table, total GW pumpage (GW_{pt} [$L\ T^{-1}$]), GW discharge (Q_{gw} [$L\ T^{-1}$]), and the change in GW storage (ΔS_g [L]) as,

$$R_{gw} - GW_{pt} - Q_{gw} = {}^{\Delta S_g}/_{\Delta t} \quad (5)$$

where Δt [T] is the model time step. The GW_{pt} is obtained as the sum of GW withdrawal for irrigation (GW_{pi}) and for water supply (domestic and industrial uses, GW_{ps}), i.e., $GW_{pt} = GW_{pi} + GW_{ps}$, where $GW_{ps} = CWU_d + CWU_i$. The ΔS_g is used to update WTD as,

$$\Delta d_{gw} = \Delta S_g / S_y \quad (6)$$

where Δd_{gw} [L] is the change in WTD updated at every time step and S_y [$L^3\ L^{-3}$] is the specific yield. Specific yield, an aquifer hydraulic parameter ranging from ~0.02 for clays to ~0.3 for coarse sands [*Fetter*, 1994], is specified in this study as a constant at 0.15 $m^3\ m^{-3}$, following its representative value averaged over the HPA [*Gutentag et al*., 1984; *Strassberg et al*., 2009]. The sensitivity test reported by *Koirala et al*. [2014] reveals that the sensitivity of specific yield to model simulations is relatively low compared to other important groundwater parameters (see equation (A3)). Moreover, even though some local data sets of specific yield exist, due to scale mismatch it is difficult to specify a single value for a large grid scale (typically ~100 km for global LSMs) based on point-scale field measurements, and is impractical to specify its global distribution. Therefore, S_y has been taken as the representative value in HPA in this study without exploring its spatial variability.

Over the long term and in the absence of pumping, the change in GW storage (ΔS_g) can be negligibly small as Q_{gw} is balanced by R_{gw}. However, the natural equilibrium is perturbed when GW is significantly pumped; if pumping is continued for a prolonged period and over an extensive area, the total amount of water released by the aquifer (pumpage plus discharge to streams and by evapotranspiration) may exceed the accumulated net GW recharge over the time resulting in persistent, and sometimes precipitous, GW depletion.

2.5. The Fully Integrated Model and Simulation Settings

The newly developed model in the fully integrated mode (a schematic is shown in Figure 1) simulates surface and subsurface water flows by taking into account the processes of runoff routing, reservoir operation,

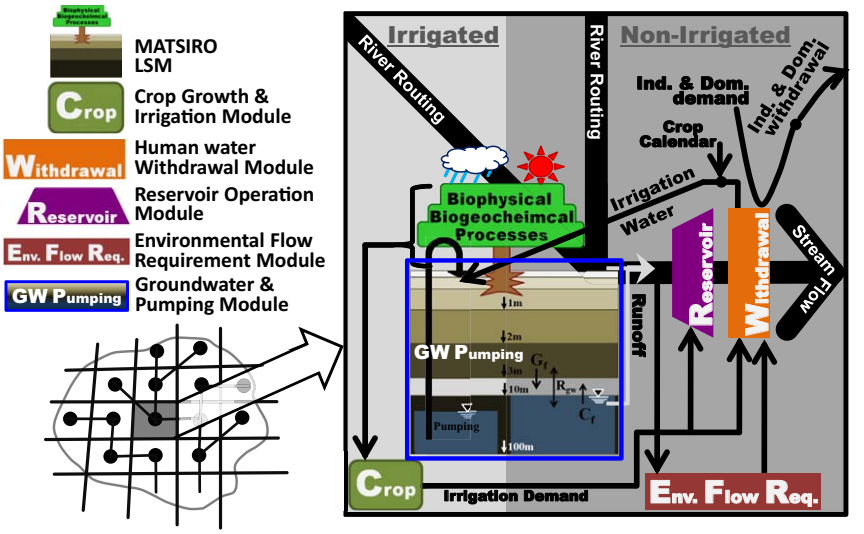

Figure 1. A schematic of the modeling framework. G_f, C_f, and R_{gw} are the gravity drainage, capillary flux, and recharge to the GW aquifer, respectively. Modified after *Pokhrel et al*. [2012b]. The blue box indicates the newly incorporated water table dynamics and groundwater pumping schemes.

irrigation, water withdrawals, environmental flow requirements, water table dynamics, and well pumping. The primary difference between the model developed by *P12b* and the new model HiGW-MAT presented here is that the imaginary source of water (NNBW) [*Rost et al*., 2008] has been replaced by the explicit representation of GW flow and pumping processes. The water demand in excess of surface water availability is extracted from the aquifer, which dynamically interacts with the overlying unsaturated zone, an important physical mechanism to exert the influence of GW pumping on the dependent hydrologic states and fluxes that was not yet represented in *P12b*.

Global simulations are conducted at the $1^\circ \times 1^\circ$ spatial resolution and an hourly time step. A 150 year spin-up run is first conducted with the repetitive forcing data for the year 1995 to reach the long-term natural dynamic equilibrium in the absence of human interventions (i.e., by turning off all human impact schemes). The fully coupled HiGW-MAT model is then run for 16 years (1995–2010) with the first 3 year simulation results discarded in the analysis to allow for the further adjustment of the water table and other state variables (soil moisture, temperature, etc.). Thus, the results from 1998 to 2010 are used for the analysis.

2.6. Data

Six-hourly climate forcing data are based on *Kim et al*. [2009]. All the default model parameters for MATSIRO and the human impact modules are identical to that used in *Takata et al*. [2003] and *P12b*, respectively, and the conceptual parameters in the GW model are based on the global parameter estimation scheme of *Koirala et al*. [2014]. Gridded irrigated areas are taken from *P12b* who developed a time series at $1^\circ \times 1^\circ$ spatial resolution based on the Global Map of Irrigated Areas (GMIA) [*Siebert et al*., 2007]. We use various in situ and satellite-based observational data to evaluate the model simulations of irrigation water requirements, groundwater withdrawal and depletion, and the variations in TWS. Country-based irrigation water requirements are based on the AQUASTAT database of the FAO (http://www.fao.org/nr/water/aquastat/main/index.stm). The global-scale groundwater withdrawal data, which are also country based, were obtained from *Wada et al*. [2010] which were compiled by using the groundwater database of the International Groundwater Resources Assessment Center (IGRAC). For the groundwater withdrawals from the principal aquifers in the U.S., we use the data collected by the USGS [*Maupin and Barber*, 2005]. For the HPA, the monthly data of soil moisture and groundwater storage were taken from *Longuevergne et al*. [2010], and the annual water level and groundwater storage data were obtained from the USGS (see details in supporting information Table S2). The USGS data were derived from well observations at more than 9000 locations throughout the HPA during winter and early spring [*McGuire*, 2011]. For the CVA, the monthly time series of groundwater storage change was obtained from *Scanlon et al*. [2012b]. We use the GRACE data from two different processing centers (Center for Space Research (CSR) and Groupe de Recherche de Géodésie

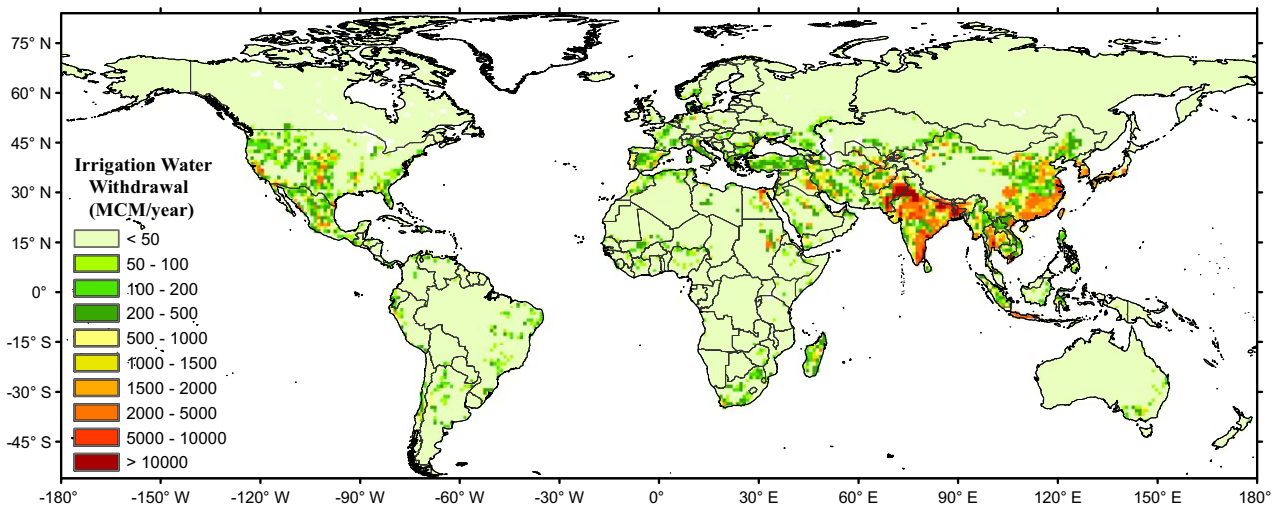

Figure 2. Simulated irrigation water withdrawals (million km^3/year) for 1° grid cells shown as the mean for the period 1998–2002.

Spatiale (GRGS)), which were processed specifically for the HPA and CVA by *Longuevergne et al*. [2010] and *Scanlon et al*. [2012b], respectively.

3. Results

3.1. River Discharge and Irrigation Water Requirement

MATSIRO has been extensively used and evaluated by various global modeling studies [e.g., *Hirabayashi et al*., 2005; *Yoshimura et al*., 2006; *Kim et al*., 2009]. These studies have demonstrated that the model reproduces observed river discharge and the variations of TWS well in most global river basins. More recently, *P12b* and *Koirala et al*. [2014] provided detailed evaluations of simulated river discharge and TWS variations over large global river basins by the MATSIRO with the human impacts and GW scheme, respectively (see Figures 2 and 3 of *P12b*, and Figure 4 of *Koirala et al*. [2014]). Here we revisit this validation to demonstrate that HiGW-MAT simulates river discharge reasonably well in the selected global river basins previously used by *P12b* and *Koirala et al*. [2014] (see supporting information Figure S2). As can be judged from this plot, the model captures the seasonal cycle fairly well. Given that the model parameters were not tuned for each individual basin, the performance over the global domain, in general, is considered to be satisfactory.

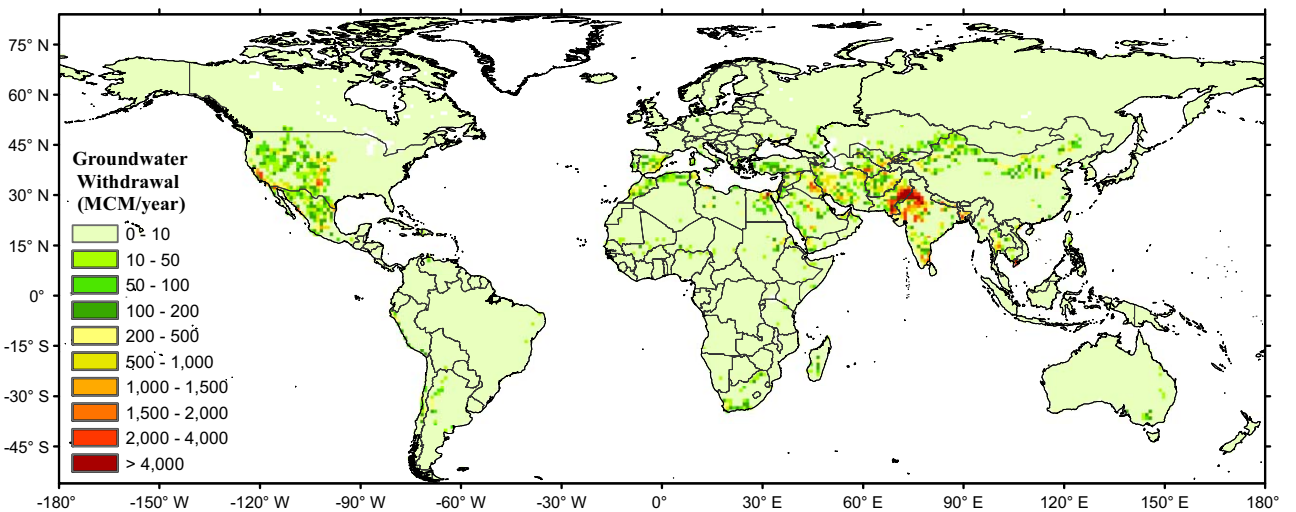

Figure 3. Simulated groundwater withdrawals (million km^3/year) for 1° grid cells shown as the mean for the period 1998–2002.

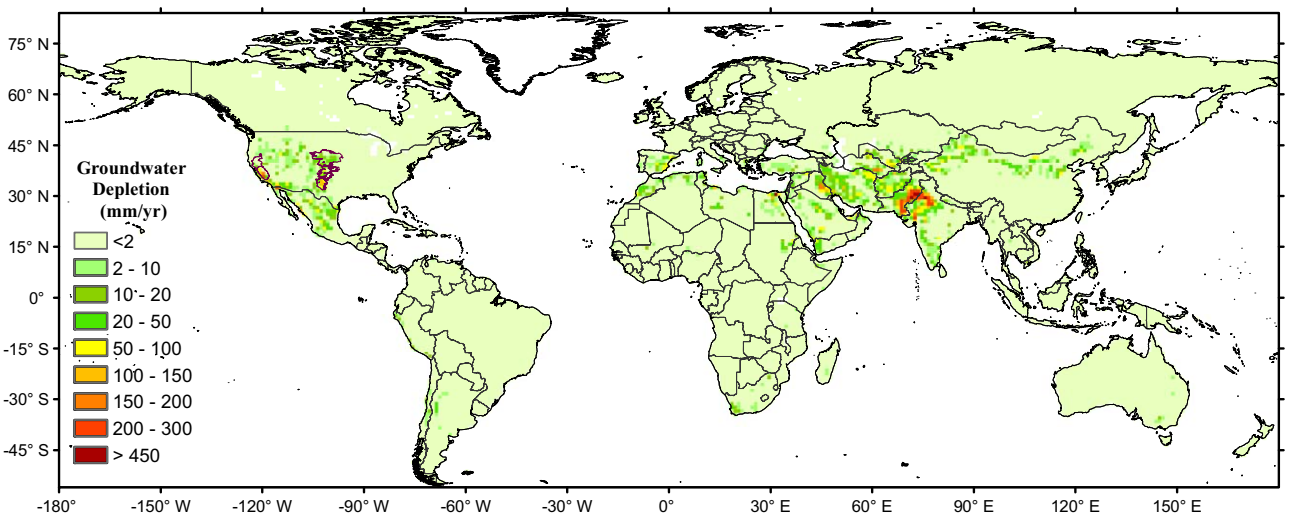

Figure 4. Simulated groundwater depletion shown as mean for the period 1998–2002.

Figure 2 presents the spatial distribution of gross irrigation water withdrawal estimated by using the simulated net (consumptive) irrigation water requirement and reported country-based irrigation efficiency [*Döll and Siebert*, 2002]. Results are shown as the mean for the 1998–2002 period to represent the conditions around year 2000 because the results of a single year could be biased due to the uncertainties in climate forcing and other data sets. As seen in the figure, the highly irrigated regions in eastern China, India, Pakistan, the Nile Delta, and central and western U.S. clearly stand out. Table 1 presents the comparison of the total volume of global irrigation water requirements simulated by HiGW-MAT with the country-based estimates by the FAO and the results of various other global hydrological models. The results of this study compare well with the previous estimates with slight overestimation compared to the FAO estimates. The global total water demand from this study is higher than that of *P12b* because the new model accounts for the GW processes which result in higher infiltration rates and the larger amounts of water that is required to maintain soil moisture near the field capacity for the optimal crop growth. Indeed, representing GW in the model notably increases evapotranspiration particularly in dry regions [*Koirala et al.*, 2014], which in turn results in higher irrigation water requirements. A country-level comparison of irrigation water withdrawals (supporting information Figure S3) indicates that the results are improved for many countries where *P12b* found an underestimation in model results compared to the FAO estimates (see Figure 4 of *P12b*).

3.2. Global GW Withdrawal and Depletion

Figure 3 depicts the simulated GW withdrawals for the year around 2000. Similar to that in Figure 2, high GW withdrawals are evident in the extensively irrigated areas, but they are small in humid regions such as the eastern parts of China and Southeast Asia where surface water availability is abundant. The simulated global total GW withdrawal is ~570 km^3 yr^{-1}. While this estimate is within the range of the previous estimates (Table 2), it may represent certain uncertainties because the model withdraws GW only if all local surface water sources are depleted to the minimum threshold required to maintain environmental flows. In reality, however, GW is used even in regions with abundant availability of surface water sources because these

Table 1. Global Total Irrigation Water Withdrawals

		Irrigation Water (km^3 yr^{-1})	
Reference	Year	Demand	Withdrawal
FAO	2000		2660
This Study	1998–2002	1238 ± 67[a]	3028 ± 171[a]
Döll and Siebert [2002]	2000	1257	3256
Rost et al. [2008]	1971–2000	1364	2555
Hanasaki et al. [2010]	2000	1598	3755
Siebert et al. [2010]	2000	1277	
Wisser et al. [2010]	2002		2997
Pokhrel et al. [2012b]	2000	1021 ± 55	2462 ± 130
Döll et al. [2012]	1998–2002	1231	3185
Wada et al. [2014]	2000	1098	2572

[a]The uncertainty represents interannual variations during 1998–2002.

Table 2. Comparison of Global Groundwater Withdrawal With Previous Studies

Reference	Year	Groundwater Withdrawal ($km^3 yr^{-1}$)
This Study	1998–2002	570 ± 61[a]
Shah et al. [2000]	Contemporary	750–800
Giordano [2009]		658
Siebert et al. [2010]	2000	545[b]
Wada et al. [2010]	2000	734
Döll et al. [2012]	1998–2002	571

[a]The Uncertainty represents interannual variations during 1998–2002.
[b]Only for irrigation.

sources are not always accessible and generally less dependable than groundwater due to the large temporal variability [*Giordano*, 2009; *Schwartz and Ibaraki*, 2011; *Aeschbach-Hertig and Gleeson*, 2012]. Such areas with underestimated GW use may include the humid regions where the model simulates abundant river flows. Thus, for instance, the model simulates very little GW withdrawal in the eastern U.S. and eastern China where the reported statistics indicate larger GW withdrawals [*Wada et al.*, 2010].

The availability of consistent and reliable GW data at the global scale is limited due to the lack of GW monitoring networks [*Giordano*, 2009; *Shah et al.*, 2007]. The best available data are the country statistics, which have been used by some studies to generate a grid-based compilation of global groundwater withdrawals and depletion [e.g., *Siebert et al.*, 2010; *Wada et al.*, 2010]. However, even these most comprehensive data suffer from high uncertainty since these studies have either applied certain data filling and extrapolation techniques or used the hydrologic model simulations to supplement the data. Our results compare fairly well with the data produced by *Wada et al.* [2010] for most countries (supporting information Figure S4), but it should be noted that *Wada et al.* [2010] reported an uncertainty of ~11% for the global total groundwater withdrawals and up to 25% for certain countries. Given the large uncertainty in the reported GW data and considering the fact that it is difficult to evaluate global model simulations, the reported statistics indeed provide useful lower and upper bounds to ensure that our model results are within the plausible limits.

Figure 4 presents the global distribution of the simulated mean annual GW depletion, i.e., annual GW withdrawal in excess of GW recharge (supporting information Figure S5) [see *Koirala* et al., 2014, for further details] for the 1998–2002 period. The global total GW depletion is estimated as ~330 $km^3 yr^{-1}$, which is substantially lower than our previously estimated NNBW of ~450 $km^3 yr^{-1}$ [*Pokhrel et al.* 2012a, 2012b], and compares better with the results of other modeling studies (e.g., 283 ± 40 $km^3 yr^{-1}$ of *Wada et al.* [2010], 257 $km^3 yr^{-1}$ of *Döll et al.* [2012], and 204 ± 30 $km^3 yr^{-1}$ of *Wada et al.* [2012]) as well as the inventory of GW depletion compiled by using the available datasets for the major aquifers around the world (~145 $km^3 yr^{-1}$ of *Konikow* [2011]). The GW withdrawal is higher than the NNBW simulated by the model without GW pumping [*P12b*] primarily because of the increased irrigation water withdrawals, but the net GW depletion is smaller than NNBW because part of the withdrawal is replenished by the increased GW recharge associated with irrigation return flows.

It is evident from Figure 4 that the largest depletion occurs in the extensively irrigated regions in northwestern India, parts of Pakistan, the Nile Delta, and the HPA and the CVA in the U.S., which are the major hot spots of GW depletion reported by various studies based on either in situ and GRACE satellite-based observations or documented statistics [e.g., *Rodell et al.*, 2009; *Wada et al.*, 2010; *Scanlon et al.*, 2012a; *Strassberg et al.*, 2009].

3.3. GW Withdrawals in the Principal Aquifers in the U.S.

Because of the limited availability of global-scale groundwater data, we focus our analysis on the principal aquifers in the U.S. for which the USGS provides the data for groundwater withdrawals [e.g., *Maupin and Barber*, 2005] and depletion [e.g., *McGuire*, 2011] on a regular basis. Here we discuss GW withdrawals in five of these aquifers: the HPA, CVA, Basin and Range Basin-Fill aquifer (BRF), Snake River Plain Basaltic-Rock aquifer (SRP), and California Coastal Basins (CCB) aquifer, which are located in the relatively dry regions, and in many of them GW levels have been continuously declining due to GW overexploitation [e.g., *Famiglietti et al.*, 2011; *Strassberg et al.*, 2009; *Scanlon et al.*, 2012a, 2012b]. GW depletion is discussed only for the HPA and CVA which rank the first and second largest respectively among the aquifers in the U.S. for total GW withdrawals, and

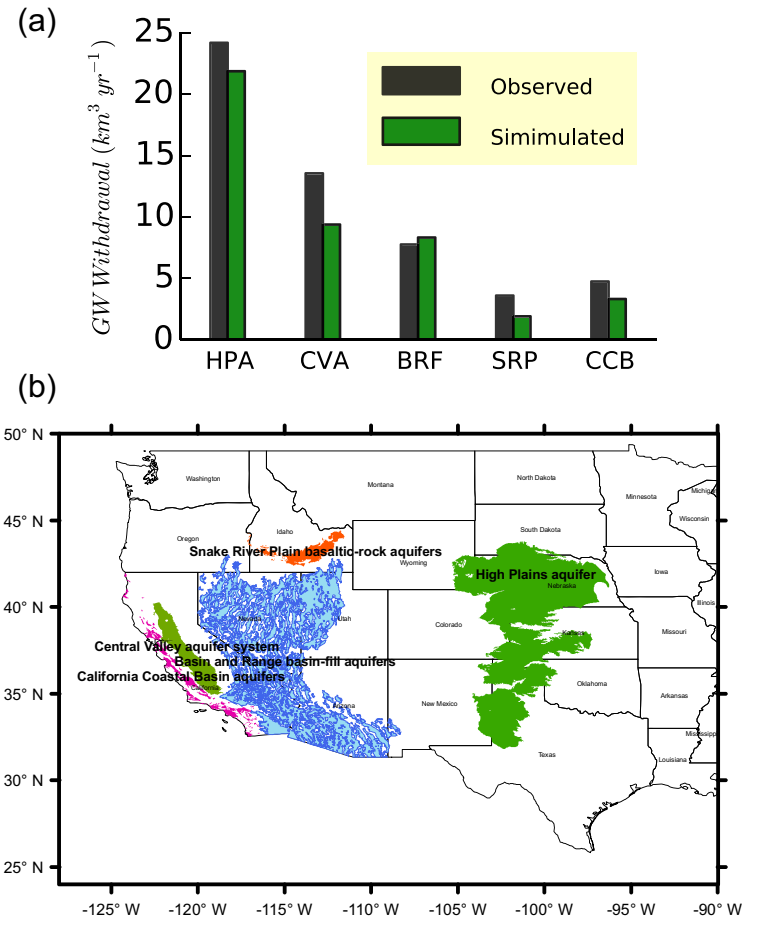

Figure 5. (a) Comparison of simulated total groundwater withdrawals from the selected principal aquifers in the U.S. with the observations. The abbreviations HPA, CVA, BRF, SRP, and CCB denote the High Plains, Central Valley, Basin and Range Basin-fill, Snake River Plain, and California Coastal Basins Aquifers, respectively, which are shown in (b).

account for more than half of the total GW depletion in the U.S. [*Maupin and Barber*, 2005; *Konikow*, 2013].

As depicted in Figure 5a, the model correctly simulates GW withdrawals in the selected five aquifers (Figure 5b) with slight underestimation except for the BRF. The overestimation in the BRF could be attributed to the overrepresentation of the aquifer area in the model grid resolution resulting from the irregular shape of small units spread over an extensive area (Figure 5b). Even though the results compare well for the CVA, SRP, and CCB aquifers, they may contain certain uncertainties because these aquifers are relatively small in size and comprise of irregularly shaped and rather small aquifer systems spread over a large area, which are difficult to accurately delineate at the 1° model grid resolution.

3.4. TWS and GW Levels in the HPA

The HPA is the most intensively exploited aquifer in the U.S. which supplies irrigation water in the High Plains where ~27% of the total irrigated lands in the nation are located. In terms of the amount of GW withdrawals, HPA accounts for ~23% of the total water withdrawals and ~30% of the total irrigation withdrawals from all aquifers in the U.S. [*Maupin and Barber*, 2005]. The extensive irrigation with large-scale pumping began during the 1940s resulting in the dramatic increase in GW withdrawals until 1980s [*McGuire*, 2011]. In recent years, GW withdrawals have generally remained stable due to the stabilized irrigated areas and improved irrigation technologies, but the GW levels have continued to decline because crop evaporation largely exceeds precipitation during the growing season [*McGuire*, 2011]. The climate in the High Plains is largely semiarid with average annual precipitation of ~500 mm [*Scanlon et al.*, 2012a]. Thus, because the annual potential evapotranspiration ranges from 1500 mm in north to 2700 mm in the

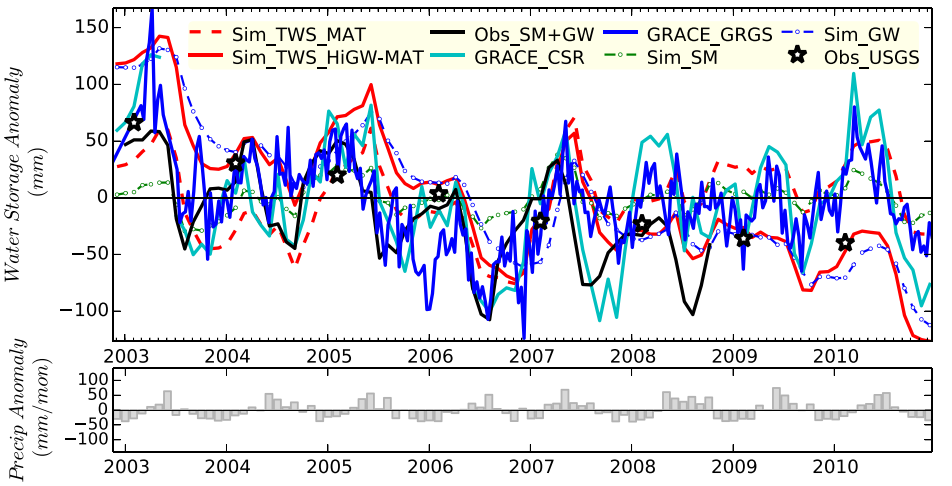

Figure 6. Comparison of simulated TWS anomalies with in situ observations and GRACE data from two different processing centers: CSR (monthly) and GRGS (10 day) averaged over the High Plains. While the simulated changes in total TWS are shown for two different model runs: MAT (only MATSIRO LSM) and the fully integrated model HiGW-MAT, the individual components are shown for HiGW-MAT only. Sim_SM and Sim_GW denote the changes in simulated root-zone (2 m) soil moisture and groundwater, respectively; surface water storage components such as snow water and water in river channels are not shown as their relative contributions are small. All plots are shown as anomalies relative to the mean for the analysis period (2003–2010). The bottom figure plots monthly precipitation anomaly.

south, most of the precipitation is returned to the atmosphere by evapotranspiration still leaving significant deficit in the supply of water which is withdrawn from the aquifer [*Rodell and Famiglietti*, 2002].

The total GW withdrawal in 2000 was reported to be ~24 $km^3\ yr^{-1}$ [*Maupin and Barber*, 2005]. Our model estimate of ~22 $km^3\ yr^{-1}$ (Figure 5a) for the 1998–2002 period is in close agreement with the reported number. Our simulation results suggest that GW withdrawals account for ~70% of the total water use in the High Plains region and nearly all of the GW is used for irrigation. Results also indicate that the annual GW withdrawal from the HPA did not show an increasing trend during the study period but it varied significantly from year to year as governed mainly by the meteorological conditions (see supporting information Table S1). The withdrawals in excess of recharge, however, resulted in the continuous depletion of GW storage. The simulated mean annual GW withdrawal for the 2001–2008 (1998–2010) period is 21.14 (20.73) km^3/yr with the depletion rate being ~10.57 (10.18) $km^3\ yr^{-1}$ which compares well with the observational record of 10.22 $km^3\ yr^{-1}$ [*Konikow*, 2013].

The model also reproduces the broad spatial patterns of GW depletion in the HPA with a clear north-south contrast (higher rate of depletion in the south; Figures 4 and S6) as revealed by the in situ well observations [*McGuire*, 2011; *Scanlon et al*., 2012a]. While the annual rate of depletion in the northern parts of the aquifer is generally less than 50 mm, some southern regions around the Texas Pan Handle suffered from a larger depletion of up to 150 mm. The southern High Plains receives very little recharge compared to the northern parts [*Scanlon et al*., 2012a] and a recent study has shown that the current spatial trend in recharge from north to south will get further amplified due to climate change [*Crosbie et al*., 2013]. This suggests that the southern regions could suffer from even larger depletion under the projected future climate.

Figure 6 plots the changes in the modeled TWS and its components averaged over the High Plains along with the TWS from GRACE satellite and the soil moisture and GW storages from in situ observations (see section 2.6). It is evident from the figure that the simulated total TWS (red) shows a declining trend which is largely due to the decline in GW storage (dashed blue) because soil moisture (dashed green) does not show any trend over the same period. The changes in surface water components (river water and snow) are not shown as their contributions to total TWS are relatively small for the High Plains [see also *Strassberg et al*., 2009]. Note that the simulated soil moisture shown in Figure 6 represents the water in the root zone (top 2 m); the rest of the subsurface storage is accounted in GW storage. We use 2 m depth to calculate the soil moisture as opposed to using the entire soil above the WTD suggested by *Pokhrel et al*. [2013] in order to avoid confusion caused by the inverse relationship between WTD-based soil moisture and GW storages. The total soil water in entire unsaturated zone is shown in supporting information Figure S7 which provides

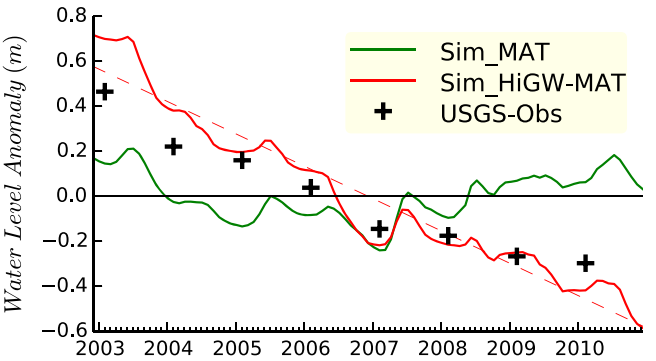

Figure 7. Comparison of simulated monthly water table depth with the observed water level change in the HPA. Simulated results from two different runs are shown: MAT (only MATSIRO LSM) and the fully integrated model HiGW-MAT. The dashed line shows the linear trend for HiGW-MAT results. Data shown are the anomalies relative to the mean for the period 2003–2010.

all water balance components for the High Plains. As seen in the figure, the unsaturated zone soil water exhibits an increasing trend due to the expansion of the unsaturated zone associated with decline in the water table.

As seen in Figure 6, the model captures the overall pattern of the TWS variations from 2003 to 2008 indicated by two different GRACE products, but it simulates a continued storage decline during 2009–2010 as opposed to the large recovery indicated by the GRACE data. To isolate the effects of human activities, we conducted a separate run by using the MATSIRO model with GW, i.e., by disabling all human impacts modules including pumping (hereafter the MAT run; dashed red in Figure 6). The results of the MAT run do not show any decline in TWS during the simulation period.

Simulated changes in TWS are in better agreement with the observed changes in subsurface water storage (soil moisture + GW: black) than with the GRACE TWS even though the observations could not confirm the case of 2009 and 2010 as the well observations extended only up to October 2008. Also shown in Figure 6 are the annual GW storage measurements published by the USGS [*McGuire*, 2011] (see section 2.6 and supporting information Table S2). These USGS observations were made once or twice a year, mostly in winter or early spring when irrigation wells typically are not pumping and water levels generally have recovered from pumping during the previous irrigation season [*McGuire*, 2011]. Therefore, we plot these values on February. As seen, the annual-level changes in the simulated GW storage agree well with USGS observations, adding further confidence to our simulations. During 2009–2010, the USGS observations do not indicate any increase in GW; given that the variations in the total TWS mostly come from the changes in GW storage, the increase in TWS in GRACE data is not expected. We note that the GRACE data are not as reliable as the in situ observations because of the inherent uncertainties in data processing which is evident from the large differences between the two different GRACE products shown in Figure 6.

A steep decline in GW storage can be seen during 2003 and 2006 which are both dry years receiving less-than-average precipitation of ∼407 and ∼466 mm, respectively (see bottom plot of Figure 6 and supporting information Table S1). The GW storage continued to decline from late 2005 until the end of 2006 owing to large GW withdrawal in 2006 (∼28 $km^3\ yr^{-1}$ compared to 1998–2010 average of ∼20 $km^3\ yr^{-1}$). It should be noted that soil moisture increased during mid-2006 while GW storage kept declining because the GW removed from the aquifer is added to the top soil as irrigation. Additionally, because the memory of soil moisture is shorter than that of GW, it responds faster to rainfall resulting in an earlier peak than GW (Figure 6). GW recovered substantially in 2007 as a result of smaller withdrawal and then remained generally uniform from 2008 to mid-2010 before it declined again during the 2010 growing season due to the low rainfall (Figure 6). As seen in Table S1, precipitation and GW withdrawal exhibit an opposite relationship in general; for the 1998–2010 period, the correlation coefficient is −0.6. These results suggest that the changes in GW storage in the HPA are determined mainly by the amount of withdrawals which is directly influenced by the meteorological conditions, particularly the amount of annual precipitation. This feature is prevalent across the highly irrigated regions in the High Plains in which a large portion of pumped GW is lost to the atmosphere through consumptive use by crops resulting in net decline in GW storage [see also *Stanton et al.*, 2011].

As simulated by HiGW-MAT, the GW levels in the HPA continuously dropped from 2003 to 2010 at an average rate of ∼14 cm yr^{-1} with certain recoveries in wet years such as 2005 and 2007 (Figure 7). These results are generally consistent with the annual-level observational records of the GW storage change published by the USGS (shown as "+" signs in Figure 7; also see Table S2 and section 2.6). The underestimated groundwater recharge and irrigation return flows could be some of the factors causing larger-than-

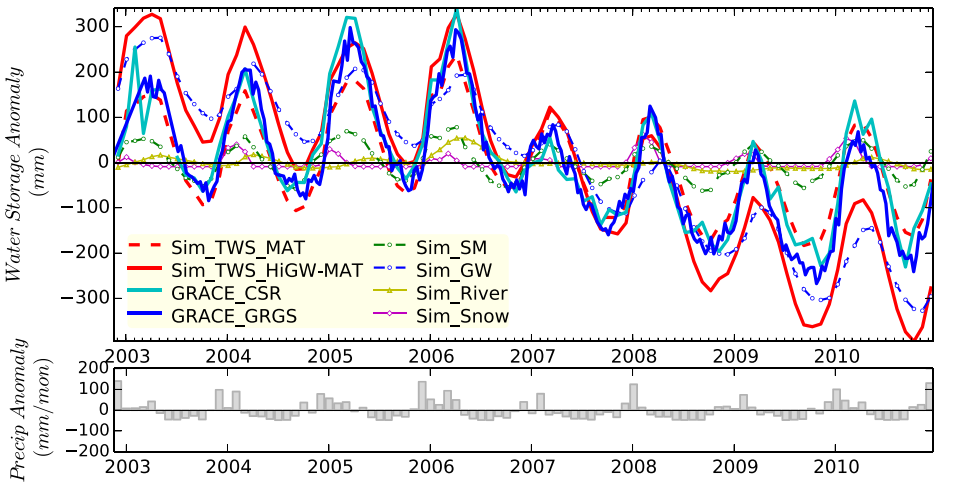

Figure 8. Comparison of simulated TWS anomalies for the Central Valley region (averaged over the combined area of Sacramento and San Joaquin river basins) with GRACE data from two processing centers: CSR (monthly) and GRGS (10 day). Sim_SM, Sim_GW, Sim_River, and Sim_Snow denote the changes in simulated root-zone (2 m) soil moisture, groundwater, river water, and snow water, respectively. While the simulated changes in total TWS are shown for two different model runs: MAT (only MATSIRO LSM) and the fully integrated model HiGW-MAT, the individual components are shown for HiGW-MAT only. The bottom figure plots monthly precipitation anomaly.

observed groundwater depletion. Simulated groundwater recharge averaged over the High Plains is ~30 mm yr^{-1} which is in the lower side of the range (19–97 mm yr^{-1}) suggested by *Scanlon et al.* [2006]. In the absence of pumping, GW levels did not show any long-term trend; the water table declined slightly during 2003–2006 but recovered completely during 2007–2010 (green line in Figure 7). These results from the model without pumping portray a dynamic steady state of GW systems over long time scales and under the influence of the climatological conditions alone. The results from HiGW-MAT, however, do not show any sign of recovery over the 8 year period. Returning back to Figure 6, it is important to note that the large recovery in TWS indicated by the GRACE data is not seen in the USGS water level observations, and this adds further confidence to our model results.

3.5. TWS and GW Levels in the CVA

Figure 8 plots the TWS and its components averaged over the combined area of Sacramento and San Joaquin river basins (~154,000 km^2) which include the Central Valley. This larger region is selected because the area of Central Valley alone (~52,000 km^2) is smaller than the GRACE footprint of ~200,000 km^2 [*Yeh et al.*, 2006]. While the total TWS remained relatively stable during 2003–2004 and increased during 2005–2006, a clear declining trend can be observed from 2007 which was triggered by the 2007 drought that persisted until 2009 [*Jones*, 2010] (supporting information Table S2). Overall, the model is generally consistent with the temporal patterns of TWS observed by GRACE except for the larger storage depletion in the model during 2009–2010. Again, the results from the MAT run seem to agree better with GRACE data, particularly for the 2009–2010 period which, however, is not supported by the observed water table data (Figure 9).

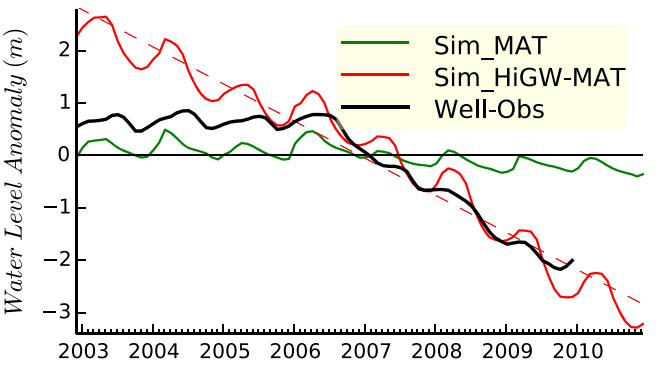

Figure 9. Comparison of simulated monthly anomaly of water table depth with the observed water level change averaged over the CVA. Simulated results are shown for two different model runs: MAT (only MATSIRO LSM) and the fully integrated model HiGW-MAT. The dashed line shows the linear trend for HiGW-MAT results.

The partitioning of the simulated total TWS into its components indicates that the declining trend in the TWS is mainly due to the depletion of GW storage caused by GW withdrawal which is eventually lost

through evapotranspiration. The climate in the Central Valley is arid to semiarid with an average precipitation of ~500 mm yr^{-1} (supporting information Table S2), which is not sufficient to fulfill the evaporative demand. Before the development of GW irrigation systems, which began around the mid-1800s, the hydrologic system in the CVA was in a dynamic steady state; the water balance was largely characterized by evapotranspiration almost equaling precipitation causing negligible changes in GW storage [*Faunt*, 2009]. As irrigated areas and facilities expanded significantly after the development GW systems, evapotranspiration increased substantially exceeding the annual precipitation in the typical and dry years resulting in the net depletion of GW within the valley [see *Faunt*, 2009, Figure B1].

According to HiGW-MAT, the average GW withdrawal from the CVA during 1998–2010 is ~10 km^3 yr^{-1} which accounted for ~90% of the withdrawal within the two river basins (supporting information Table S2). During the analysis period (2003–2010), the largest GW depletion occurred during 2006–2007 (Figure 8) due to the combined effects of low precipitation and high GW withdrawal in 2007, the driest year in the analysis period (~436 mm compared to 1998–2010 average of 610 mm yr^{-1}). However, the GW withdrawal did not attain its maximum value in 2007 because of the carryover in soil and GW storages from the preceding year which was relatively wet. As the drought persisted through 2008 and 2009, the GW withdrawals dramatically increased and attained their highest values (both ~16 km^3 yr^{-1}) that resulted in continued GW depletion until it stabilized in 2010 as a result of significantly higher precipitation of ~755 mm yr^{-1}. Along with the GW storage, surface water storage (yellow line in Figure 8) also declined appreciably in 2006 and did not recover until 2010, indicating that surface water storages remained below average during the drought years. However, the contribution of the changes in surface water storages to the total TWS variations is relatively small as opposed to the large surface water storage contributions (about one-third of the total TWS depletion) suggested by *Famiglietti et al*. [2011]. This underestimation of surface water storage in our model could be attributed partly to the underrepresentation of reservoirs because only the large reservoirs (>1 km^3) were taken into account [see *Hanasaki et al*., 2006; *P12b*]. Soil moisture and snow did not represent any declining trends over the analysis period which is in line with the conclusion of *Famiglietti et al*. [2011]. A detailed plot showing all water balance components averaged over the Central Valley is provided in the supporting information (Figure S7).

Simulated results indicate that the water table in the CVA declined at the rate of ~71 cm yr^{-1} from 2003 to 2010 (Figure 9) with a steep decline after the onset of drought in late 2006. Note that the simulated WTD anomaly has been scaled by the specific yield of 0.177, an average value for the CVA suggested by *Scanlon et al*. [2012b], because the specific yield used in the model was 0.15. The interannual changes in GW level are consistent with the well observations [*Scanlon et al*., 2012b] for the 2006–2009 period, but the model overestimates the rate of water level decline prior to 2006. For the 2003–2006 period, the results of MAT run show a similar pattern to that of observations suggesting that our model might have overestimated GW withdrawal and depletion for this period. However, the simulated changes in GW level during 2003–2004 are consistent with the below-average precipitation and typical annual withdrawals (supporting information Table S2). Moderate-to-wet climate and the associated lower withdrawals during 2005–2006 kept the GW levels relatively stable. The model overestimation of the water table decline could generally be attributed to two primary factors. First, recharge to the aquifer could have been underestimated due to the missing processes such as the topography-driven lateral GW flow and focused GW recharge from streambeds or other mountainous sources. As *Faunt* [2009] indicated CVA receives a notable fraction of recharge from the surrounding mountains; this could also partially explain the discrepancies between the observed and simulated depletion rate during 2003–2006. Second, other possible factors that affect local groundwater use such as long-distance water transfer and nonstructural methods of water saving employed during drought years are not represented in the model which, to some extent, could have led to the high GW withdrawals and consequently the larger depletion.

4. Summary and Conclusions

In this study, we develop an integrated hydrologic model which explicitly simulates GW dynamics and pumping within the framework of a global LSM that also accounts for human activities such as irrigation and reservoir operation. In the new model, which builds upon our previous modeling efforts, we replace the conceptual model for obtaining water from an imaginary source to always fulfill the demand by an

explicit GW pumping scheme that links human water use and GW dynamics; thus, the GW withdrawals and the associated changes in GW storage are explicitly simulated within a single, internally consistent modeling framework. This provides a unique opportunity for studying the dynamic relationship between human water use and the changes in GW storage as well as the associated climate impacts and feedbacks, particularly in regions where the GW systems are being depleted due to overexploitation.

Comparison of the simulated irrigation water requirements, GW withdrawal, and GW depletion with the available observations indicates that the model reproduces the global total volumes of these important entities within the plausible limits. Because GW storage data are scarce at the global scale, the present study focused on the principal aquifers in the U.S. which are relatively data rich in terms of GW monitoring. Simulated results of GW withdrawal in most of the selected aquifers in the western U.S. are found to be consistent with the reported data. Moreover, in situ and GRACE satellite observations are used to evaluate the simulated GW storage depletion. In the HPA, the model simulates a continuous decline in GW levels at an average rate of $\sim$14 cm yr^{-1} during 2003–2010, which is in line with the observational data. It is also found that GW supplies more than 70% of the total water use in the regions overlying the HPA, most of which is used for irrigation. During the same period, the simulated water table in the CVA declined at an average rate of $\sim$71 cm yr^{-1} which is in close agreement with the observed decline during mid-2006 to 2009 but is much larger than the observed change during 2003–2006.

While the newly developed model accounts for various important aspects of human water use and GW dynamics, there are still certain limitations which need to be addressed in the future works. Some important issues include refining the model grid resolution, constraining the irrigation based on actual irrigation practices, setting physical constraints on GW withdrawal, and incorporating lateral GW flow and intergrid water transfer processes, among others. As suggested by a recent study [*Krakauer et al*., 2014], the effect of topography-driven lateral groundwater flow is relatively insignificant in global models with grid sizes of $\sim$100 km, but as the spatial resolution increases, representation of lateral flow may become indispensable in order to simulate the topography-driven spatial redistribution of subsurface water and hence to accurately represent subgrid heterogeneity of the WTD, as discussed in various previous studies [e.g., *Fan et al*., 2007; *Ferguson and Maxwell*, 2012; *Condon and Maxwell*, 2014]. Thus, despite its important significance in small-scale and high-resolution applications, the role of lateral GW flow may, however, not be critical in the present study because the major focus is on the long-term and large-scale water balance including pumping rather than the short-term temporal dynamics. Evaluation of model results against observations in all global regions of GW overexploitation is also necessary to add more confidence to our results. This is of particular importance in order to improve our result of GW depletion which is larger than other estimates. A synthesis of reliable GW data [e.g., *Scanlon et al*., 2006; *Fan et al*., 2013], as it becomes increasingly available for more global regions of GW overexploitation, will facilitate such model evaluations and improvements in the future.

Despite these limitations, this study provides a way forward by accounting for the important processes of GW dynamics and well pumping that are missing in most global-scale land surface and hydrologic models. There are several important implications of the present work. First, the developed modeling framework is a useful tool for quantifying the contributions of various natural and anthropogenic factors that alter the hydrological cycle. Second, while the present study discussed the results from offline simulations, the LSM can also be coupled to its parent GCM to assess potential climate impacts and feedbacks due to anthropogenic disturbance of the terrestrial water cycle. For example, the coupled model can be used to trace the flow paths of the pumped GW in order to estimate its fraction that flows to global oceans causing sea level rise [*Pokhrel et al*., 2012a]. The model can also be used to study the observed impacts of irrigation pumping on regional climate [e.g., *DeAngelis et al*., 2010]. Third, the model could be a useful tool for the projection of future water resources and to study the sustainability of GW resources in regions where GW systems are being depleted at an alarming rate. In light of the increasing concerns about human interventions on the water cycle, this study contributes to advance the representation of GW dynamics and well pumping within the framework of global climate models.

Appendix A

The GW scheme consists of an unconfined aquifer model (described in *Koirala et al*. [2014]) in which the soil column has explicit representations of both the unsaturated soil zone and the underlying unconfined

aquifer which interact continuously through an exchange of moisture flux near the water table. The water balance equation for the aquifer can be expressed as,

$$S_y \frac{\Delta d_{gw}}{\Delta t} = R_{gw} - Q_{gw} \tag{A1}$$

where, S_y [L^3 L^{-3}] is the specific yield, d_{gw} [L] is the WTD, R_{gw} [L T^{-1}] is GW recharge to (positive) or capillary rise from (negative) the GW reservoir, and Q_{gw} [L T^{-1}] is base flow. The R_{gw} is estimated by using physically-based Darcy's law as the sum of downward gravity drainage and upward capillary flux as,

$$R_{gw} = K_u \left[\frac{d\psi}{dz} - 1 \right] \tag{A2}$$

where K_u [L T^{-1}] is the unsaturated hydraulic conductivity of soil, $d\psi$ [L] is the difference between the matric potentials of saturated aquifer and unsaturated soil layer, and dz [L] is the distance between water table and center of the lowermost unsaturated soil layer.

The base flow is estimated by using a threshold relationship developed by *Yeh and Eltahir* [2005a] based on observations in Illinois as,

$$Q_{gw} = \begin{cases} K(d_0 - d_{gw}); & 0 \le d_{gw} < d_0 \\ 0; & d_{gw} \ge d_0 \end{cases} \tag{A3}$$

where, K [T^{-1}] is the outflow constant, and d_0 [L] is the threshold WTD; base flow is initialized if d_{gw} is shallower than the threshold. Both d_0 and d_{gw} are taken as positive values. Details of the implementation of these equations into MATSIRO, the estimation of global parameters and their physical interpretations, and the validation of results with the observed river discharge in the large global river basins can be found in *Koirala et al*. [2014]. Both d_0 and d_{gw} are conceptual parameters which cannot be measured directly and are required to be calibrated against observed streamflow. We use the global parameters estimated by *Koirala et al*. [2014] that were obtained by transferring the optimal parameters for the Illinois to global regions by using precipitation climatology. Note that the lateral groundwater flow is not accounted in the present study because the significance of lateral flow may not be obvious at the model grid scale of ~100 km [*Krakauer et al*., 2014]. Moreover, the major objective of the present study is to simulate the long-term and large-scale patterns of groundwater storage change rather than to reproduce the subgrid variability of the WTD and the topography-induced spatial redistribution of subsurface water.

Acknowledgments

We would like to thank Bridget Scanlon for providing with the data for the CVA. We also thank Hyungjun Kim for the forcing data. The study was partially supported by the Ministry of Education, Culture, Sports, Science, and Technology (MEXT), Japan and the Japan Society for the Promotion of Science KAKENHI, Grant-in-Aid for Scientific Research (S) (23226012). Different data set used for model evaluation was obtained from various sources described in section 2.6. While the irrigation and groundwater withdrawal data can be downloaded freely from the FAO website (http://www.fao.org/nr/water/aquastat/main/index.stm), the other data should be obtained from the authors of the references provided in the paper.

References

Aeschbach-Hertig, W., and T. Gleeson (2012), Regional strategies for the accelerating global problem of groundwater depletion, *Nat. Geosci.*, *5*, 853–861.

Alcamo, J., P. Döll, T. Henrichs, F. Kaspar, B. Lehner, T. Rösch, and S. Siebert (2003), Development and testing of the WaterGAP 2 global model of water use and availability, *Hydrol. Sci. J.*, *48*, 317–337.

Alkama, R., B. R. Decharme, H. Douville, M. Becker, A. Cazenave, J. Sheffield, A. Voldoire, S. Tyteca, and P. Le Moigne (2010), Global evaluation of the ISBA-TRIP continental hydrological system. Part I: Comparison with GRACE terrestrial water storage estimates and in situ river discharges, *J. Hydrometeorol.*, *11*, 583–600.

Alley, W. M., R. W. Healy, J. W. LaBaugh, and T. E. Reilly (2002), Hydrology-flow and storage in groundwater systems, *Science*, *296*, 1985–1990.

Alsdorf, D. E., and D. P. Lettenmaier (2003), Tracking fresh water from space, *Science*, *301*, 1491–1494.

Beven, K. J., and M. J. Kirkby (1979), A physically based variable contributing area model of basin hydrology, *Hydrol. Sci. Bull.*, *24*, 43–69.

Collatz, G., J. T. Ball, C. Grivet, and J. A. Berry (1991), Physiological and environmental regulation of stomatal conductance, photosynthesis and transpiration: A model that includes a laminar boundary layer, *Agric. For. Meteorol.*, *54*, 107–136.

Condon, L. E., and R. M. Maxwell (2014), Feedbacks between managed irrigation and water availability: Diagnosing temporal and spatial patterns using an integrated hydrologic model, *Water Resour. Res.*, *50*, 2600–2616, doi:10.1002/2013WR014868.

Crosbie, R. S., B. R. Scanlon, F. S. Mpelasoka, R. C. Reedy, J. B. Gates, and L. Zhang (2013), Potential climate change effects on groundwater recharge in the High Plains Aquifer, USA, *Water Resour. Res.*, *49*, 3936–3951, doi:10.1002/wrcr.20292.

de Rosnay, P., J. Polcher, K. Laval, and M. Sabre (2003), Integrated parameterization of irrigation in the land surface model ORCHIDEE, Validation over Indian Peninsula, *Geophys. Res. Lett.*, *30*(19), 1986, doi:10.1029/2003GL018024.

DeAngelis, A., F. Dominguez, Y. Fan, A. Robock, M. D. Kustu, and D. Robinson (2010), Evidence of enhanced precipitation due to irrigation over the Great Plains of the United States, *J. Geophys. Res.*, *115*, D15115, doi:10.1029/2010JD013892.

Döll, P., and S. Siebert (2002), Global modeling of irrigation water requirements, *Water Resour. Res.*, *38*(4), doi:10.1029/2001WR000355.

Döll, P., H. Hoffman-Dobrev, F. T. Portmann, S. Siebert, A. Eicker, M. Rodell, G. Strassberg, and B. R. Scanlon (2012), Impact of water withdrawals from groundwater and surface water on continental water storage variations, *J. Geodyn.*, *59-60*, 143–156.

Döll, P., H. Müller Schmied, C. Schuh, F. T. Portmann, and A. Eicker (2014), Global-scale assessment of groundwater depletion and related groundwater abstractions: Combining hydrological modeling with information from well observations and GRACE satellites, *Water Resour. Res.*, *50*, 5698–5720, doi:10.1002/2014WR015595.

Famiglietti, J., M. Lo, S. Ho, J. Bethune, K. Anderson, T. Syed, S. Swenson, C. de Linage, and M. Rodell (2011), Satellites measure recent rates of groundwater depletion in California's central valley, *Geophys. Res. Lett.*, *38*, L03403, doi:10.1029/2010GL046442.

Fan, Y., G. Miguez-Macho, C. P. Weaver, R. Walko, and A. Robock (2007), Incorporating water table dynamics in climate modeling: 1. Water table observations and the equilibrium water table simulations, *J. Geophys. Res.*, *112*, D10125, doi:10.1029/2006JD008111.

Fan, Y., H. Li, and G. Miguez-Macho (2013), Global patterns of groundwater table depth, *Science*, *339*(6122), 940–943.

Faunt, C. C. (Ed.) (2009), Groundwater availability of the Central Valley Aquifer, California, *U.S. Geol. Surv. Prof. Pap.*, 1766, 173 pp.

Ferguson, I. M., and R. M. Maxwell (2012), Human impacts on terrestrial hydrology: Climate change versus pumping and irrigation, *Environ. Res. Lett.*, *7*, 044022.

Fetter, C. W. (1994), *Applied Hydrogeology*, 3rd ed., Prentice Hall, Upper Saddle River, N. J.

Foster, S. S. D., and P. J. Chilton (2003), Groundwater: The processes and global significance of aquifer degradation, *Philos. Trans. R. Soc. B*, *358*, 1957–1972.

Giordano, M. (2009), Global groundwater? Issues and solutions, *Annu. Rev. Environ. Resour.*, *34*, 153–178.

Gleeson, T., Y. Wada, M. Bierkens, and P. Ludovicus (2012), Water balance of global aquifers revealed by groundwater footprint, *Nature*, *488*, 197–200.

Gleick, P. H. (2003), Global freshwater resources: Soft-Path solutions for the 21st century, *Science*, *302*(5650), 1524–1528.

Gleick, P. H., and M. Palaniappan (2010), Peak water limits to freshwater withdrawal and use, *Proc. Natl. Acad. Sci. U. S. A.*, *107*, 11,155–11,162.

Gutentag, E. D., F. J. Heimes, N. C. Krothe, R. R. Luckey, and J. B. Weeks (1984), Geohydrology of the High Plains aquifer in parts of Colorado, Kansas, Nebraska, New Mexico, Oklahoma, South Dakota, Texas, and Wyoming, *U.S. Geol. Surv. Prof. Pap., 1400-B*, 66 pp.

Haddeland, I., T. Skaugen, and D. P. Lettenmaier (2006), Anthropogenic impacts on continental surface water fluxes, *Geophys. Res. Lett.*, *33*, L08406, doi:10.1029/2006GL026047.

Hanasaki, N., S. Kanae, and T. Oki (2006), A reservoir operation scheme for global river routing models, *J. Hydrol.*, *327*, 22–41.

Hanasaki, N., S. Kanae, T. Oki, K. Masuda, K. Motoya, N. Shirakawa, Y. Shen, and K. Tanaka (2008), An integrated model for the assessment of global water resources—Part 1: Model description and input meteorological forcing, *Hydrol. Earth Syst. Sci.*, *12*, 1007–1025.

Hanasaki, N., T. Inuzuka, S. Kanae, and T. Oki (2010), An estimation of global virtual water flow and sources of water withdrawal for major crops and livestock products using a global hydrological model, *J. Hydrol.*, *384*, 232–244.

Hasumi and Emori (2004), K-1 coupled model (MIROC) description, K-1 technical report, 34 pp., Cent. for Clim. Syst. Res., Univ. of Tokyo, Tokyo, Japan.

Hirabayashi, Y., S. Kanae, I. Struthers, and T. Oki (2005), A 100-year (1901–2000) global retrospective estimation of the terrestrial water cycle, *J. Geophys. Res.*, *110*, D19101, doi:10.1029/2004JD005492.

Jackson, R. B., S. R. Carpenter, C. N. Dahm, D. M. McKnight, R. J. Naiman, S. L. Postel, and S. W. Running (2001), Water in a changing world, *Ecol. Appl.*, *11*, 1027–1045.

Jones, J. (2010), *California's Drought of 2007–2009: An Overview*, vol. 1, 116 pp., Nat. Resour. Agency, Calif. Dep. of Water Resour., Calif.

Kim, H., P. J.-F. Yeh, T. Oki, and S. Kanae (2009), Role of rivers in the seasonal variations of terrestrial water storage over global basins, *Geophys. Res. Lett.*, *36*, L17402, doi:10.1029/2009GL039006.

Koirala, S., P. J.-F. Yeh, Y. Hirabayashi, S. Kanae, and T. Oki (2014), Global-scale land surface hydrologic modeling with the representation of water table dynamics, *J. Geophys. Res. Atmos.*, *119*, 75–89, doi:10.1002/2013JD020398.

Konikow, L. F. (2011), Contribution of global groundwater depletion since 1900 to sea-level rise, *Geophys. Res. Lett.*, *38*, L17401, doi: 10.1029/2011GL048604.

Konikow, L. F. (2013), Groundwater depletion in the United States (1900−2008), *U.S. Geol. Surv. Sci. Invest. Rep.*, 2013−5079, 63 p.

Konikow, L. F., and E. Kendy (2005), Groundwater depletion: A global problem, *Hydrogeol. J.*, *13*, 317–320.

Krakauer, N. Y., H. Li, and Y. Fan (2014), Groundwater flow across spatial scales: Importance for climate modeling, *Environ. Res. Lett.*, *9*, 034003.

Krysanova, V., D.-I. Müller-Wohlfeil, and A. Becker (1998), Development and test of a spatially distributed hydrological/water quality model for mesoscale watersheds, *Ecol. Modell.*, *106*, 261–289.

Leng, G., M. Huang, Q. Tang, W. J. Sacks, H. Lei, and L. R. Leung (2013), Modeling the effects of irrigation on land surface fluxes and states over the conterminous United States: Sensitivity to input data and model parameters, *J. Geophys. Res. Atmos.*, *118*, 9789–9803, doi: 10.1002/jgrd.50792.

Lettenmaier, D. P., and J. S. Famiglietti (2006), Water from on high, *Nature*, *444*, 562–563.

Lo, M., and J. Famiglietti (2010), Effect of water table dynamics on land surface hydrologic memory, *J. Geophys. Res.*, *115*, D22118, doi: 10.1029/2010JD014191.

Lo, M.-H., and J. S. Famiglietti (2013), Irrigation in California's Central Valley strengthens the southwestern U.S. water cycle, *Geophys. Res. Lett.*, *40*, 301–306, doi:10.1002/grl.50108.

Longuevergne, L., B. R. Scanlon, and C. R. Wilson (2010), GRACE hydrological estimates for small basins: Evaluating processing approaches on the high plains aquifer, USA, *Water Resour. Res.*, *46*, W11517, doi:10.1029/2009WR008564.

Maupin, M. A., and N. L. Barber (2005), Estimated withdrawals from principal aquifers in the United States, 2000, *U.S. Geol. Surv. Circ.*, 1279, 46 pp.

Maxwell, R. M., and N. L. Miller (2005), Development of a coupled land surface and groundwater model, *J. Hydrometeorol.*, *6*, 233–247.

McGuire, V. L. (2011), Water-level changes in the High Plains aquifer, predevelopment to 2009, 2007–08, and 2008–09, and change in water in storage, predevelopment to 2009, *U.S. Geol. Surv. Sci. Invest. Rep.*, 2011–5089, 13 pp.

Miguez-Macho, G., and Y. Fan (2012), The role of groundwater in the Amazon water cycle: 1. Influence on seasonal streamflow, flooding and wetlands, *J. Geophys. Res.*, *117*, D15113, doi:10.1029/2012JD017539.

Morris, B. L., A. R. L. Lawrence, P. J. C. Chilton, B. Adams, R. C. Calow, and B. A. Klinck (2003), *Groundwater and Its Susceptibility to Degradation: A Global Assessment of the Problem and Options for Management, Early Warning Assess. Rep. Ser.*, vol. 03-3, 126 pp., U. N. Environ. Prog., Nairobi.

Nilsson, C., C. A. Reidy, M. Dynesius, and C. Revenga (2005), Fragmentation and flow regulation of the World's Large River Systems, *Science*, *308*, 405–408.

Niu, G.-Y., Z.-L. Yang, R. E. Dickinson, L. E. Gulden, and H. Su (2007), Development of a simple groundwater model for use in climate models and evaluation with Gravity Recovery and Climate Experiment data, *J. Geophys. Res.*, *112*, D07103, doi:10.1029/2006JD007522.

Oki, T., and S. Kanae (2006), Global hydrological cycles and world water resources, *Science*, *313*, 1068–1072.

Oki, T., and Y. Sud (1998), Design of Total Runoff Integrating Pathways (TRIP)–A global river channel network, *Earth Interact.*, *2*, 1–37.

Ozdogan, M., M. Rodell, H. K. Beaudoing, and D. L. Toll (2010), Simulating the effects of irrigation over the United States in a land surface model based on satellite-derived agricultural data, *J. Hydrometeorol.*, *11*, 171–184.
Pokhrel, Y., N. Hanasaki, P. Yeh, T. Yamada, S. Kanae, and T. Oki (2012a), Model estimates of sea-level change due to anthropogenic impacts on terrestrial water storage, *Nat. Geosci.*, *5*, 389–392.
Pokhrel, Y., N. Hanasaki, S. Koirala, J. Cho, H. Kim, P. J.-F. Yeh, S. Kanae, and T. Oki (2012b), Incorporating anthropogenic water regulation modules into a land surface model, *J. Hydrometeorol.*, *13*, 255–269.
Pokhrel, Y. N., Y. Fan, G. Miguez-Macho, P. J.-F. Yeh, and S.-C. Han (2013), The role of groundwater in the Amazon water cycle: 3. Influence on terrestrial water storage computations and comparison with GRACE, *J. Geophys. Res. Atmos.*, *118*, 3233–3244, doi:10.1002/jgrd.50335.
Postel, S., G. Daily, and P. Ehrlich (1996), Human appropriation of renewable fresh water, *Science*, *271*, 785–788.
Postel, S. L. (1999), *Pillars of Sand: Can the Irrigation Miracle Last?*, W. W. Norton, N. Y.
Richards, L. A. (1931), Capillary conduction of liquids through porous mediums, *Physics*, *1*, 318–333.
Rockström, J., et al. (2009), A safe operating space for humanity, *Nature*, *461*, 472–475.
Rodell, M., and J. S. Famiglietti (2002), The potential for satellite-based monitoring of groundwater storage changes using GRACE: The High Plains aquifer, central U.S., *J. Hydrol.*, *263*, 245–256.
Rodell, M., et al. (2004), The Global Land Data Assimilation System, *Bull. Am. Meteorol. Soc.*, *85*(3), 381–394, doi:10.1175/BAMS-85-3-381.
Rodell, M., I. Velicogna, and J. S. Famiglietti (2009), Satellite-based estimates of groundwater depletion in India, *Nature*, *460*, 999–1002.
Rosegrant, W. M., and X. Cai (2002), Global water demand and supply projections. Part 2: Results and prospects to 2025, *Water Int.*, *27*(3), 170–181.
Rost, S., D. Gerten, A. Bondeau, W. Lucht, J. Rohwer, and S. Schaphoff (2008), Agricultural green and blue water consumption and its influence on the global water system, *Water Resour. Res.*, *44*, W09405, doi:10.1029/2007WR006331.
Sahagian, D., F. Schwartz, and D. Jacobs (1994), Direct anthropogenic contributions to sea level rise in the twentieth century, *Nature*, *367*, 54–57.
Scanlon, B. R., K. E. Keese, A. L. Flint, L. E. Flint, C. B. Gaye, W. M. Edmunds, and I. Simmers (2006), Global synthesis of groundwater recharge in semiarid and arid regions, *Hydrol. Processes*, *20*, 3335–3370.
Scanlon, B. R., C. C. Faunt, L. Longuevergne, R. C. Reedy, W. M. Alley, V. L. McGuire, and P. B. McMahon (2012a), Groundwater depletion and sustainability of irrigation in the US High Plains and Central Valley, *Proc. Natl. Acad. Sci. U. S. A.*, *109*(24), 9320–9325.
Scanlon, B. R., L. Longuevergne, and D. Long (2012b), Ground referencing GRACE satellite estimates of groundwater storage changes in the California Central Valley, USA, *Water Resour. Res.*, *48*, W04520, doi:10.1029/2011WR011312.
Schwartz, F. W., and M. Ibaraki (2011), Groundwater: A resource in decline, *Elements*, *7*, 175–179, doi:10.2113/gselements.7.3.175.
Shah, T., D. Molden, R. Sakthivadivel, and D. Seckler (2000), *Global Groundwater Situation: Opportunities and Challenges*, Int. Water Manage. Inst., Colombo.
Shah, T., J. Burke, and K. Villholth (2007), Groundwater: A global assessment of scale and significance, in *Water for Food, Water for Life*, edited by D. Molden, pp. 395–423, Earthscan, London, U. K.
Shiklomanov, I. A. (2000), Appraisal and assessment of world Water Resources, *Water Int.*, *25*, 11–32.
Siebert, S., P. Döll, S. Feick, J. Hoogeveen, and K. Frenken (2007), *Global Map of Irrigation Areas Version 4.0.1*, Univ. of Frankfurt (Main), Frankfurt, Germany.
Siebert, S., J. Burke, J. M. Faures, K. Frenken, J. Hoogeveen, P. Döll, and F. T. Portmann (2010), Groundwater use for irrigation—A global inventory, *Hydrol. Earth Syst. Sci.*, *14*, 1863–1880.
Sophocleous, M. (2002), Interactions between groundwater and surface water: The state of the science, *Hydrogeol. J.*, *10*(1), 52–67.
Sorooshian, S., J. Li, K.-L. Hsu, and X. Gao (2011), How significant is the impact of irrigation on the local hydroclimate in California's Central Valley? Comparison of model results with ground and remote-sensing data, *J. Geophys. Res.*, *116*, D06102, doi:10.1029/2010JD014775.
Stanton, J. S., S. L. Qi, D. W. Ryter, S. E. Falk, N. A. Houston, S. M. Peterson, S. M. Westenbroek, and S. C. Christenson (2011), Selected approaches to estimate water-budget components of the high plains, 1940 through 1949 and 2000 through 2009, *U.S. Geol. Surv. Sci. Invest. Rep.*, 2011–5183, 79 pp.
Stieglitz, M., D. Rind, J. Famiglietti, and C. Rosenzweig (1997), An efficient approach to modeling the topographic control of surface hydrology for regional and global climate modeling, *J. Clim.*, *10*, 118–137.
Strassberg, G., B. Scanlon, and D. Chambers (2009), Evaluation of groundwater storage monitoring with the GRACE satellite: Case study of the high plains aquifer, central United States, *Water Resour. Res.*, *45*, W05410, doi:10.1029/2008WR006892.
Takata, K., S. Emori, and T. Watanabe (2003), Development of the minimal advanced treatments of surface interaction and runoff, *Global Planet. Change*, *38*, 209–222.
Tapley, B. D., S. Bettadpur, J. C. Ries, P. F. Thompson, and M. M. Watkins (2004), GRACE measurements of mass variability in the Earth system, *Science*, *305*, 503–505.
Taylor, R. G., et al. (2013), Ground water and climate change, *Nat. Clim. Change*, *3*(4), 322–329.
van Beek, L. P. H., Y. Wada, and M. F. P. Bierkens (2011), Global monthly water stress: 1. Water balance and water availability, *Water Resour. Res.*, *47*, W07517, doi:10.1029/2010WR009791.
Voisin, N., H. Li, D. Ward, M. Huang, M. Wigmosta, and L. R. Leung (2013), On an improved sub-regional water resources management representation for integration into earth system models, *Hydrol. Earth Syst. Sci.*, *17*, 3605–3622.
Vörösmarty, C. J., P. Green, J. Salisbury, and R. B. Lammers (2000), Global water resources: Vulnerability from climate change and population growth, *Science*, *289*, 284–288.
Wada, Y., L. P. H. van Beek, C. M. van Kempen, J. W. T. M. Reckman, S. Vasak, and M. F. P. Bierkens (2010), Global depletion of groundwater resources, *Geophys. Res. Lett.*, *37*, L20402, doi:10.1029/2010GL044571.
Wada, Y., L. P. H. van Beek, D. Viviroli, H. H. Dürr, R. Weingartner, and M. F. P. Bierkens (2011), Global monthly water stress: 2. Water demand and severity of water stress, *Water Resour. Res.*, *47*, W07518, doi:10.1029/2010WR009792.
Wada, Y., L. P. H. vanBeek, F. C. Sperna Weiland, B. F. Chao, Y.-H. Wu, and M. F. P. Bierkens (2012), Past and future contribution of global groundwater depletion to sea-level rise, *Geophys. Res. Lett.*, *39*, L09402, doi:10.1029/2012GL051230.
Wada, Y., D. Wisser, and M. F. P. Bierkens (2014), Global modeling of withdrawal, allocation and consumptive use of surface water and groundwater resources, *Earth Syst. Dyn.*, *5*, 15–40.
Watanabe, T. (1994), Bulk parameterization for a vegetated surface and its application to a simulation of nocturnal drainage flow, *Boundary Layer Meteorol.*, *70*, 13–35.
Watanabe, M., et al. (2010), Improved climate simulation by MIROC5: Mean states, variability, and climate sensitivity, *J. Clim.*, *23*(23), 6312–6335.

Wisser, D., B. M. Fekete, C. J. Vörösmarty, and A. H. Schumann (2010), Reconstructing 20th century global hydrography: A contribution to the Global Terrestrial Network-Hydrology (GTN-H), *Hydrol. Earth Syst. Sci.*, *14*, 1–24.

Wood, E. F., et al. (2011), Hyperresolution global land surface modeling: Meeting a grand challenge for monitoring Earth's terrestrial water, *Water Resour. Res.*, *47*, W05301, doi:10.1029/2010WR010090.

Yeh, P. J. F., and E. A. B. Eltahir (2005a), Representation of water table dynamics in a land surface scheme. Part I: Model development, *J. Clim.*, *18*, 1861–1880.

Yeh, P. J. F., and E. A. B. Eltahir (2005b), Representation of water table dynamics in a land surface scheme. Part II: Subgrid variability, *J. Clim.*, *18*, 1881–1901.

Yeh, P. J.-F., S. C. Swenson, J. S. Famiglietti, and M. Rodell (2006), Remote sensing of GW storage changes in Illinois using the Gravity Recovery and Climate Experiment (GRACE), *Water Resour. Res.*, *42*, W12203, doi:10.1029/2006WR005374.

Yeh, P. J. F., and J. S. Famiglietti (2009), Regional groundwater evapotranspiration in Illinois, *J. Hydrometeorol.*, *10*, 464–478.

Yoshimura, K., S. Miyazaki, S. Kanae, and T. Oki (2006), Iso-MATSIRO, a land surface model that incorporates stable water isotopes, *Global Planet. Change*, *51*(1-2), 90–107.